Enhancing Spectral Color Images by RGB-Based Sharpening

Oili Kohonen, School of Computing, University of Eastern Finland, Joensuu, Finland

Abstract

This work examines a possibility to enhance the spatial resolution of spectral color images by using RGB color images. NuanceFX spectral imaging system, which allows the measuring of both spectral and RGB color images at different resolution levels using the identical geometry, is used for acquiring the images needed. The used enhancing process is based on the correspondence between spectra of a low spatial resolution spectral image, LR_{SPE}*, and RGB-triplets of a high spatial resolution RGB image,* HR_{RGB}*, both globally and locally. In a global approach, an estimated spectrum corresponding to index number* i *is defined as the average of all the spectra mapping into that index number, whereas in a local approach an estimated spectrum is defined as a spectrum of the closest mother pixel with the same index number. In the cases where the index number of pixel to be estimated equals to zero, the missing spectrum is estimated based on its neighborhood. The estimated high resolution spectral images,* EHR_{SPE}*, are evaluated by comparing them to the real, measured high resolution spectral images,* HR_{SPE}*, with respect to RMS errors and* ΔE^*_{ab} *color differences under four different CIE illuminants,* D_{65}*, A, F8 and F11.*

Introduction

Spectral imaging allows gathering of information that may be invisible to the image capturing techniques relying on the principle of trichromatic theory. In comparison to the conventional metameric imaging, the use of spectral imaging increases the accuracy of the acquired data. Spectral imaging, however, is more time consuming than imaging employing only the commonly used three channels, R, G and B. In addition to other factors such as the power of the used illumination and the physical properties of the used camera system, the time needed for acquiring a spectral image is dependent on desired spatial and spectral resolution. The higher the degree of the details, the more time is expended on acquiring process. However, in many imaging applications both high spectral and high spatial resolution are required simultaneously, which puts challenges both to readout implementation and data processing [1].

In the area of remote sensing a fusion technique called pansharpening is often used. Pansharpening techniques aim to increase the spatial resolution while simultaneously preserving the spectral information in the spectral data [2]. In practise, pansharpening techniques combine panchromatic images of high spatial resolution, HR_{PAN}, and spectral images of low spatial resolution, LR_{SPE}, in order to generate spectral images of high spatial resolution, HR_{SPE}.

The aim of this work is to examine whether the idea of pansharpening could be applied for spectral color images in order to decrease the amount of data to be processed during the acquiring phase. Instead of a spectral image of high spatial resolution, a spectral image of low spatial resolution and an RGB image of high spatial resolution could be acquired and later be combined into a spectral image of high spatial resolution. Despite of wide range of proposed techniques, there exists no ideal fusion method and the fused images are thought as tradeoffs between a good geometrical representation of structures and a good representation of original colors [3]. Therefore, the enhancing process used in this study is based on the correspondence between spectra of low spatial resolution spectral image, LR_{SPE}, and RGB-triplets of high spatial resolution RGB image, HR_{RGB}, both globally and locally.

The generated spectral images of high resolution images, EHR_{SPE}, are evaluated by comparing them to the real high resolution spectral images, HR_{SPE}, acquired using the identical measuring geometry with respect to both RMS errors and ΔE^*_{ab} color differences. The ΔE^*_{ab} color difference calculations are performed under CIE illuminants, D_{65}, A, F8 and F11 by using CIE 1964 Supplementary Standard Colorimetric Observer [4].

Resolution Enhancement

RGB-based enhancing of spectral images spatial resolution exploits the relationship between spectral images of low spatial resolution and RGB-images of high spatial resolution. When talking about resolution, one can mean both spatial and spectral resolution. However, throughout this paper, word resolution will always refer on spatial resolution and thus, the resolution enhancement means increase in spatial resolution.

Preprocessing: registration

Image registration ensures that information, coming from images acquired from different viewpoints with various sensors and possible different times, refers to the same physical region [5]. Mis-registrations cause artificial colors and features falsifying the interpretation and thus registration is an important preprocessing step in image fusion [2]. A large variety of different registration techniques have been developed and the existing algorithms are often classified according to their nature (area- based and feature-based) and according to four basic steps of image registration procedure: feature detection, feature matching, mapping function design, and image transformation and re-sampling [5]. In this work, however, all the used images have been acquired using the same spectral imaging system and the same measuring geometry, so the registration phase is pretty straightforward and complex registration techniques are not needed.

Replacing mother pixels

After registration phase, the corresponding pixels in a high resolution RGB-image, HR_{RGB}, and a low resolution spectral image, LR_{SPE}, are found, and a table consisting of connections between RGB-triplets and color spectra is generated. These corresponding pixels are from now on referred as mother pixels. In the case of low resolution image all original pixels belong to mother pixels. At the first step of the enhancing process each mother pixel in a low resolution image is replaced with n child pixels, of which one is identical to the mother pixel and the others are initialized to zero. The pixel preserving the original, acquired spectral information is never modified during the later

phases of the enhancing process. Thus, the enhancing process can be considered as adding the extra pixels between the original mother pixels. The mother pixels could also be considered as averages of the child pixels, and could thus be replaced at the beginning with four equal child pixels. That approach would, however, cause the undesired loss of the original spectral data. An example of the relationships between the original low resolution spectral image and the generated high resolution spectral image in the case of fourfold enhancement is shown in Fig. 1.

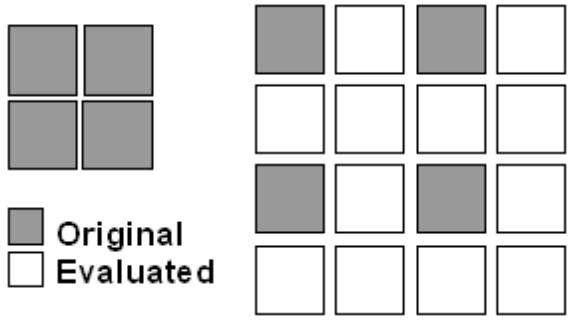

Figure 1. *The relationships between the original* $\mathrm{LR_{SPE}}$ *(left) and the generated* $\mathrm{EHR_{SPE}}$ *(right).*

After replacing the mother pixels with child pixels, the spectral properties of the zero-initialized child pixels are estimated based on the low resolution spectral image (mother pixels) and the high resolution RGB-image. From now on the enhancing process can be divided into three steps, which are

1. Generating a high resolution index image
2. Mapping acquired spectra to index numbers
3. Estimating spectra of non-preserving child pixels

A flowchart of the generation of a high resolution spectral image is shown in Fig. 2. The steps presented in the flowchart are explained in more detail below.

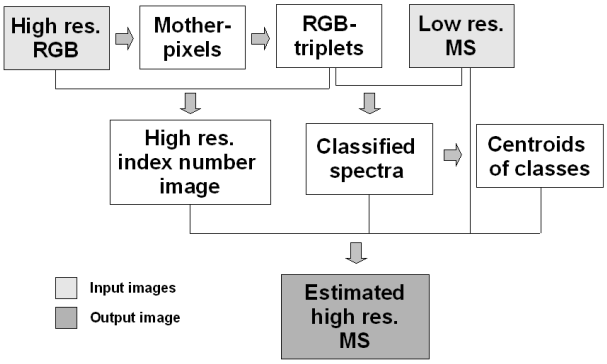

Figure 2. *A flowchart of the generation of a high resolution spectral image.*

Generating a high resolution index image

Generating of a high resolution index image is the first step in a real enhancing process. Those RGB triplets, whose physical location corresponds to pixels of $\mathrm{LR_{SPE}}$, are collected from a $\mathrm{HR_{RGB}}$ and indexed such that each index number corresponds to one triplet, and vice versa. An index number image is generated by replacing each triplet of the original $\mathrm{HR_{RGB}}$ by it's index number. Pixels not corresponding to the locations of $\mathrm{LR_{SPE}}$ may contain such triplets which are not included into the collected triplets, and in these cases the index numbers are set to 0. An example of the generation of an index number image is shown in Fig. 3. An original $\mathrm{HR_{RGB}}$ is shown on the left and the table of its index numbers in the middle. The resulting index number image is shown on the right.

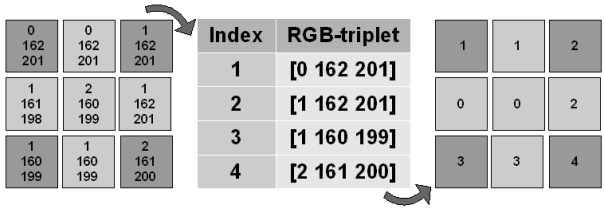

Figure 3. *A high resolution image with original RGB-triplets, a table of indexed RGB-triplets (middle), and the generated index number image (right). Mother-pixels are colored with darker gray.*

Estimating spectra of non-preserving child pixels

The estimation of the spectra to be added is based on two approaches, and the choice of approach depends on the index number of the pixel to be estimated. For index numbers differing from zero there exist one or more so called reference spectra whereas for index number equaling to zero such reference spectra does not exist. A flowchart of the used estimation approaches shown in Fig. 4. For practical reasons, the estimation of pixels with nonzero index number is proceeded before the pixels whose index number equals to zero.

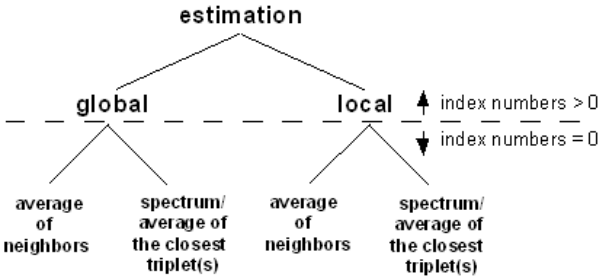

Figure 4. *A flowchart of the used estimation approaches.*

The estimation of pixels with nonzero index number is performed either globally or locally. In global approach, the estimated spectrum $\tilde{\mathrm{S}}(\lambda)$ corresponding to index number i is defined as the average of all the spectra mapping into that index number,

$$\tilde{S}(\lambda) = \frac{1}{m}\sum_{k=1}^{n} S_k(\lambda) u_{ki}. \qquad (1)$$

where n is the number of spectra in image, $\mathrm{S_k}(\lambda)$ is the $\mathrm{k^{th}}$ spectrum, $\mathrm{u_{ki}}$ is a scalar value assigned to 1, if $\mathrm{S_k}(\lambda)$ belongs to group of $\mathrm{i^{th}}$ index number, otherwise it has a zero value, and m is the number of non-zero $\mathrm{u_{ki}}$ values. The processing of global approach consumes less time than the local approach. However, the group average may not always represent well all the spectra in the group, especially in the cases of metameric pairs.

©2010 Society for Imaging Science and Technology

In a local approach the $\tilde{S}(\lambda)$ is defined as the spectrum of the closest mother pixel with the same index number. The distance D between a pixel to be estimated, P_1, and a candidate pixel, P_2, is defined as Manhattan distance,

$$D = \sum_{i=1}^{2} |P_{1i} - P_{2i}|. \quad (2)$$

In local approach, the estimated spectrum $\tilde{S}(\lambda)$ corresponding to index number i is defined as,

$$\tilde{S}(\lambda) = \frac{1}{m} \sum_{k=1}^{n_D} S_k(\lambda) u_{ki}, \quad (3)$$

where n_D is the number of pixels at the distance D from the pixel to be estimated, u_{ki} is a scalar value assigned to 1, if $S_k(\lambda)$ belongs to group of i^{th} index number, otherwise it has a zero value, and m is the number of non-zero u_{ki} values. An example of the distances between the red pixel to be estimated and its neighboring pixels are shown in Fig. 5. Red pixel is the pixel to be estimated, gray pixels are mother pixels among which the corresponding index number are searched and the numbers define the manhattan distance from the red pixel. At first round the mother pixels at one pixel distance are gone through. If the pixel with corresponding pixel number is not found, the distance is increased by two and the mother pixels at three pixel distance are examined. If one valid mother pixel is found, the pixel to be estimated is replaced by the spectrum of this mother pixel. If more than one valid mother pixel are found at the distance D from the pixel to be estimated, the average spectrum of these mother pixels is used.

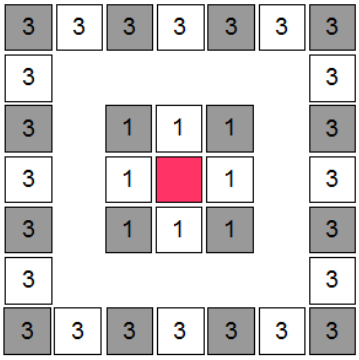

Figure 5. *The distances between the pixel to be estimated (red) and its neighboring pixels.*

In the cases where the index number of pixel to be estimated equals to zero, the missing spectrum is estimated based on its neighborhood using two different methods. In the first method the estimated spectrum, $\tilde{S}(\lambda)$, is defined as average of spectra of the best matching neighbor (BMN) in RGB space.

$$\sum_{k=1}^{3} (RGB_{0k} - RGB_{BMNk})^2 = min_i(\sum_{k=1}^{3}(X)),$$
$$X = (RGB_{0k} - RGB_{ik})^2) \quad (4)$$

in which RGB_0 is the RGB triplet of the pixel to be estimated and RGB_i is the RGB triplet of the i^{th} spectrally nonzero neighbor. Furthermore,

$$\tilde{S}(\lambda) = \frac{1}{n_{BMN}} \sum_{j=1}^{n_{BMN}} \tilde{S_{BMN_j}}(\lambda). \quad (5)$$

An example of defining $\tilde{S}(\lambda)$ is shown in Fig. 6, in which the spectrum of red pixel is to be estimated. RGB triplets of the pixel to be estimated and its neighboring pixels are shown on the left and the distances between the neighboring triplets and the triplet corresponding to the pixel to be estimated on the right. In this case there are two BMNs and these pixels are colored with green color. Now the spectrum of the red pixel is defined based on these two green pixels. The left one is a mother pixel, so one knows it already contains a spectrum. From Fig. 3 one can see that the index number of the green pixel on the right is 3 and thus differs from zero. This means that also this pixels already contains a spectrum and the $\tilde{S}(\lambda)$ can be taken as average of these two green pixels. in RGB space

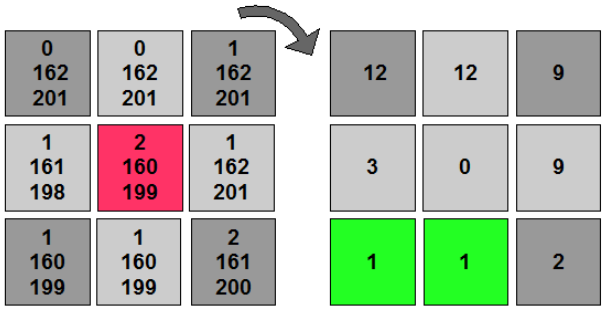

Figure 6. *The RGB neighborhood of the pixel to be estimated (left) and the distances between the neighboring triplets (right).*

In the second method, the estimated spectrum, $\tilde{S}(\lambda)$, is defined as average of the neighboring pixels,

$$\tilde{S}(\lambda) = \frac{1}{n_n} \sum_{k=1}^{n_n} S_k(\lambda), \quad (6)$$

in which n_n is the number of nonzero neighboring pixels and $S_k(\lambda)$ is k^{th} neighboring spectrum.

Experiments

Acquired images

In these experiments four objects were acquired by Nuance FX multispectral imaging system [6], which allows the measuring of both spectral and RGB color images at three resolution levels. The images were acquired with a geometry 45/0, 45 and 0 being the angles between the normal of the measured surface and the incident light, and the normal of the measured surface and the capturing device, respectively. Both spectral and RGB color images were taken at two resolution levels and the the sizes of the produced images were 520x696 and 1040x1392 pixels, respectively. The objects were measured under D_{65} light source of Gretag Macbeth SpectraLight III light booth, and in the case of spectral images the used wavelength range was from 420nm to 720nm at 20nm intervals. However, due to the low spectral radiance of the used light source at the beginning of the blue region of the spectrum and due to the possible lower sensitivity of the used camera system at the very same region, the first two channels contained too much noise and thus, were not used in the experiments. The measured objects consisted of different materials such as cardboard (”food”and ”tea”), and plastic (”deos”). The surfaces of all the other measured objects but ”deos” were flat. The measured objects are shown in an RGB format in Fig. 7.

Figure 7. *The acquired images in an RGB-format. The first row: "chart" & "deos" and the second row: "food" & "tea".*

Color differences between acquired images

In order to distinguish the color differences between the real high resolution spectral image HR_{SPE} and the estimated high resolution spectral image EHR_{SPE} into the differences originated from the discrepancy between acquired spectra at low and high resolution levels and the differences resulted in the enhancing process, the RMS errors and ΔE^*_{ab} color differences between the acquired high and low resolution spectral images were calculated. For conducting these calculations, the high resolution spectral images were transformed into the lower resolution level by using the previously defined mother-pixels instead of whole spectral image. The color difference calculations were performed under CIE illuminants D_{65}, A, F8 and F11 by using CIE 1964 Supplementary Standard Colorimetric Observer. Average and maximum RMS errors and average ΔE^*_{ab} color differences between the acquired spectral images of high and low resolution are shown in Table 1.

	Average ΔE^*_{ab} under				RMS error	
Image	D_{65}	A	F8	F11	max	ave
chart	1.6	1.5	1.5	1.8	0.0841	0.0085
deos	1.8	1.8	1.8	2.0	0.1014	0.0082
food	1.9	1.8	1.8	2.1	0.0742	0.0093
tea	1.9	1.9	1.8	2.1	0.1160	0.0100

Table 1. Average and maximum RMS errors, and average ΔE^*_{ab} color differences between the acquired HR_{SPE} and LR_{SPE} under CIE illuminants D_{65}, A, F8 and F11.

Groups

Average and maximum RMS errors and average ΔE^*_{ab} color differences between the group averages and the spectra in the groups under illuminants A, D_{65}, F8 and F11 are shown in Table 2. In M1 the used spectra are taken from HR_{SPE} and the RGB triplets from HR_{RGB} whereas in M2 the spectra are taken from LR_{SPE} and the RGB triplets are from HR_{RGB}.

Enhancing process and results achieved

The spectral images are enhanced by using the described methods. At first, the images are enhanced from the acquired low resolution spectral image and as a result, four different images are got,

1. Nonzero pixels globally & zero pixels as averages of neighbors

	Average color differences							
	under A		under D_{65}		under F8		under F11	
Image	M1	M2	M1	M2	M1	M2	M1	M2
chart	0.4	0.5	0.4	0.5	0.4	0.5	0.5	0.6
food	0.4	0.5	0.4	0.5	0.4	0.5	0.4	0.5
deos	0.4	0.5	0.4	0.5	0.4	0.5	0.5	0.5
tea	0.5	0.5	0.6	0.6	0.5	0.5	0.6	0.6
	RMS errors							
	M1				M2			
Image	max		ave		max		ave	
chart	0.0423		0.0019		0.0819		0.0024	
food	0.0238		0.0015		0.00498		0.0019	
deos	0.0252		0.0017		0.0685		0.0020	
tea	0.0821		0.0022		0.0036		0.0022	

Table 2. Average and maximum RMS errors and average ΔE^*_{ab} color differences between the group averages and the spectra in the groups under illuminants D_{65}, A, F8 and F11.

2. Nonzero pixels globally & zero pixels as spectrum/averages of the closest triplet(s)
3. Nonzero pixels locally & zero pixels as averages of neighbors
4. Nonzero pixels locally & zero pixels as spectrum/averages of the closest triplet(s).

Next, the 1/4 of the acquired high resolution images were used as low resolution spectral images and the enhancing was performed as above.

Average ΔE^*_{ab} color differences between the estimated high resolution spectral image EHR_{SPE} and the real, measured high resolution spectral image HR_{SPE} under illuminants D_{65}, A, F8 and F11 are shown in Tables 3 and 4. In the case of results shown in Table 3 the spectral images are enhanced from low resolution spectral images whereas in the case of results shown in Table 4 the 1/4 of the acquired high resolution image is used as starting point for the enhancing process. In the case of global approach the spectra of nonzero index numbers are taken as averages of spectra within group whereas in the case of local approach the spectra of nonzero index numbers are estimated locally based on the search in an increasing neighborhood. In the cases of MA and MB, the spectra of zero index numbers are taken as averages of eight neighboring pixels and as "spectra of closest RGB neighbors", respectively. The maximum and average RMS errors between the estimated high resolution spectral image EHR_{SPE} and the real, measured high resolution spectral image HR_{SPE} in the cases of enhancing from low resolution image and 1/4 of the high resolution image are shown in Tables 5 and 6.

Discussion and Conclusions

A possibility to enhance the spatial resolution of spectral color images by using RGB color images was examined in this work. The experiments were performed by using spectral and RGB color images of four objects. The used images were acquired by NuanceFX spectral imaging system and there was both low and high resolution version of each image used. The enhancing process was divided into two parts which were the estimation of pixels whose index numbers were nonzero and estimation of pixels whose index numbers were equal to zero. Furthermore, the estimation of pixels whose index numbers were nonzero was divided into two approaches. In the global approach, the estimated spectrum corresponding to index number i was defined as the average of all the spectra mapping into that index number,

©2010 Society for Imaging Science and Technology

Global approach								
	under D_{65}		under A		under F8		under F11	
Image	MA	MB	MA	MB	MA	MB	MA	MB
chart	1.5	1.6	1.5	1.5	1.5	1.6	1.7	1.8
food	2.0	2.1	1.9	2.0	1.9	2.0	2.1	2.2
deos	1.7	1.8	1.7	1.8	1.7	1.8	1.9	2.0
tea	2.2	2.2	2.2	2.3	2.1	2.2	2.3	2.4
Local approach								
	under D_{65}		under A		under F8		under F11	
Image	MA	MB	MA	MB	MA	MB	MA	MB
chart	1.6	1.6	1.5	1.5	1.6	1.5	1.8	1.8
food	2.1	2.2	2.0	2.1	2.0	2.2	2.2	2.3
deos	1.8	1.8	1.8	1.8	1.7	1.8	1.9	2
tea	2.3	2.4	2.2	2.3	2.2	2.3	2.4	2.5

Table 3. Average ΔE^*_{ab} color differences between the EHR_{SPE} and HR_{SPE} under illuminants A, D_{65}, F8 and F11. EHR_{SPE} has been enhanced from low resolution spectral image.

Global approach								
	under D_{65}		under A		under F8		under F11	
Image	MA	MB	MA	MB	MA	MB	MA	MB
chart	0.8	0.8	0.8	0.8	0.8	0.8	1.0	1.0
food	1.3	1.4	1.2	1.3	1.2	1.3	1.3	1.4
deos	1.0	1.1	1.0	1.0	1.0	1.0	1.2	1.2
tea	1.4	1.5	1.4	1.5	1.4	1.5	1.5	1.6
Local approach								
	under D_{65}		under A		under F8		under F11	
Image	MA	MB	MA	MB	MA	MB	MA	MB
chart	0.9	0.9	0.8	0.8	0.8	0.8	1.0	1.0
food	1.4	1.4	1.3	1.4	1.3	1.4	1.4	1.5
deos	1.0	1.1	1.0	1.0	1.0	1.0	1.2	1.2
tea	1.5	1.6	1.5	1.6	1.5	1.6	1.6	1.7

Table 4. Average ΔE^*_{ab} color differences between the EHR_{SPE} and HR_{SPE} under CIE illuminants D_{65}, A, F8 and F11. EHR_{SPE} has been enhanced from 1/4 of high resolution spectral image.

and in the local approach the estimated spectrum was defined as the spectrum of the closest mother pixel with the same index number. The estimation of the pixels whose index number was zero was based on the neighborhood of the pixel to be estimated. Again, two different approaches was used and the missing spectrum was defined either based on the best matching neighbor (BMN) in RGB space or average spectrum of neighboring pixels.

	RMS errors			
	Global			
	MA		MB	
Image	max	ave	max	ave
chart	0.2146	0.0086	0.2460	0.0087
food	0.0930	0.0094	0.1422	0.0099
deos	0.3301	0.0082	0.3905	0.0084
tea	0.1726	0.0112	0.2254	0.0118
	Local			
	MA		MB	
Image	max	ave	max	ave
chart	0.2328	0.0778	0.2509	0.0779
food	0.0930	0.0097	0.1422	0.0103
deos	0.1131	0.0087	0.1833	0.0086
tea	0.1746	0.0116	0.2241	0.0122

Table 5. Maximum and average RMS errors between the EHR_{SPE} and HR_{SPE} under CIE illuminants D_{65}, A, F8 and F11. EHR_{SPE} has been enhanced from low resolution spectral image.

	RMS errors			
	Global			
	MA		MB	
Image	max	ave	max	ave
chart	0.1175	0.0036	0.1423	0.0036
food	0.0967	0.0053	0.0996	0.0056
deos	0.1053	0.0038	0.1360	0.0039
tea	0.1682	0.0069	0.2345	0.0075
	Local			
	MA		MB	
Image	max	ave	max	ave
chart	0.2351	0.0778	0.2527	0.0779
food	0.0967	0.0056	0.0996	0.0060
deos	0.1052	0.0039	0.1360	0.0040
tea	0.1707	0.0075	0.2533	0.0081

Table 5. Maximum and average RMS errors between the EHR_{SPE} and HR_{SPE} under CIE illuminants D_{65}, A, F8 and F11. EHR_{SPE} has been enhanced from 1/4 of high resolution spectral image.

The images were enhanced using both the acquired low resolution spectral images and 1/4 of the acquired high resolution spectral images as a starting point. The latter enhancing was performed in order to provide some certain reference results against which the enhancing results from the previously mentioned case could be also evaluated. The generated high resolution spectral images were evaluated by comparing them to the real, measured high resolution spectral images with respect to both RMS errors and ΔE^*_{ab} color differences under four different CIE illuminants, D_{65}, A, F8 and F11. Obviously the color differences and RMS errors are smaller in the case where the 1/4 of the high resolution spectral images are used as starting points for enhancing process when compared to the cases in which the enhancing has been started from low resolution spectral images. When comparing the results of methods referred as MA and MB, the lower differences are achieved by using the method MA, in which the pixels whose index numbers equal to zero are estimated as taken as averages of neighboring pixels. The differences are not very big but the results are straightforward. The case is similar when the estimation processes of those pixels whose index numbers are nonzero are evaluated. The global approach seems to be slightly better.

In general, the proposed local approach is much more time consuming compared to the global approach and thus the use of it does not seem very tempting unless there are some reason to expect the case of metameric colors. Otherwise, the extra time spent for complete local search does not seem to be beneficial. The problem with global approach is that the spectra mapping into the same RGB triplet may vary a lot and may also contain some meaningful and important ”outliers”. In the case of global approach, this kind of information may be neglected.

This study was based on small amount of images of rather simplified objects. The work needed to be done in the future would be the examination of more challenging objects, in which the details and the areas of solid colors are very tiny. Instead of either global or local approach one should find a way how to combine the both perspectives and thus, be able to achieve rather time efficient method. Furthermore, image to be processed could be divided into parts based on a corresponding high resolution

RGB image. Based on this information parts of unified colors could be enhanced using different method than the border areas or any other complex parts.

Acknowledgements

The funding from Kordelin Foundation is gratefully appreciated.

References

[1] T. Hyvarinen, E. Herrala and A. DallAva, Direct Sight Imaging Spectrograph: a Unique Add-On Component Brings Spectral Imaging to Industrial Applications, Proc. IS&T/SPIEs Symposium on Electronic Imaging: Science and Technology (EI98), in Conference 3302: Digital Solid State Cameras: Design and Applications, (1998).

[2] C. Pohl, and J. L. van Genderen, Multisensor Image Fusion in Remote Sensing: Concepts, Methods and Applications, Int. J. Remote Sensing, 19, 823 (1998).

[3] A. Loza, T. D. Dixon, E. F. Canga, S. G. Nikolov, D. R. Bull, C. N. Canagarajah, J. M. Noyes, and T. Troscianko, Methods of Fused Image Analysis and Assessment, Advances and Challenges in Multisensor Data and Information Processing, NATO Security Through Science Series, IOS Press, 2007.

[4] CIE Publication No. 15:2004, Colorimetry, 3rd. ed., Central Bureau of the CIE, 2004.

[5] B. Zitova, and J. Flusser, Image Registration Methods: a Survey, Image and Vision Computing, 21, 977 (2003).

[6] http://www.criinc.com/products/

Author Biography

Oili Kohonen was born in 1978, in Lappeenranta, Finland. She receiver her M.Sc. and Ph.D. degrees in physics in 2002 and 2007 from the University of Joensuu, Finland.

©2010 Society for Imaging Science and Technology